

Review

# A Comprehensive Review of Fatigue Strength in Pure Copper Metals (DHP, OF, ETP)

Eduardo Jiménez-Ruiz <sup>1</sup>, Rubén Lostado-Lorza <sup>2</sup> and Carlos Berlanga-Labari <sup>1,\*</sup>

<sup>1</sup> Department of Engineering, Institute for Advanced Materials and Mathematics (INAMAT2), Public University of Navarra—UPNA, Campus Arrosadía S/N, 31006 Pamplona, Spain; eduardo.jimenez@unavarra.es

<sup>2</sup> Department of Mechanical Engineering, University of La Rioja, 26004 Logroño, Spain; ruben.lostado@unirioja.es

\* Correspondence: carlos.berlanga@unavarra.es

**Abstract:** Due to their exceptional electrical and thermal conductivity properties, high-purity copper (Cu-DHP) and copper alloys of similar composition, such as electrolytic tough-pitch (ETP), oxygen-free electronic (OFE) and oxygen-free (OF), have often been used in the manufacture of essential components for the electrical, electronic and power generation industries. Since these components are subject to cyclic loads in service, they can suffer progressive structural damage that causes failure due to fatigue. The purpose of this review is to examine the most relevant aspects of mechanical fatigue in Cu-DHP, ETP, OFE and OF. The impact of many factors on fatigue strength ( $S_e$ ), including the frequency, temperature, chemical environment, grain size, metallurgical condition and load type, were analyzed and discussed. Stress–life (S-N) curves under zero mean stress ( $\sigma_m = 0$ ) were found for high-cycle fatigue (HCF). For non-zero mean stress ( $\sigma_m \neq 0$ ), stress curves were based on a combination of Gerber, Soderberg and ASME elliptic failure criteria. Stress–life (S-N) curves were also developed to correlate fatigue strength ( $S_e$ ) with stress amplitude ( $\sigma_a$ ), yield strength ( $S_{yp}$ ) and ultimate strength ( $S_{ut}$ ). Finally, for low-cycle fatigue (LCF), strain–life ( $\epsilon$ -N) curves that establish a relationship between the number of cycles to failure (N) and total strain amplitude ( $\epsilon_{plastic}$ ) were determined. Hence, this review, as well as the proposed curves, provide valuable information to understand fatigue failure for these types of materials.

**Keywords:** pure copper metals; high-cycle fatigue; low-cycle fatigue; Cu-DHP



**Citation:** Jiménez-Ruiz, E.; Lostado-Lorza, R.; Berlanga-Labari, C. A Comprehensive Review of Fatigue Strength in Pure Copper Metals (DHP, OF, ETP). *Metals* **2024**, *14*, 464. <https://doi.org/10.3390/met14040464>

Academic Editor: Matteo Benedetti

Received: 29 February 2024

Revised: 30 March 2024

Accepted: 9 April 2024

Published: 15 April 2024



**Copyright:** © 2024 by the authors. Licensee MDPI, Basel, Switzerland. This article is an open access article distributed under the terms and conditions of the Creative Commons Attribution (CC BY) license (<https://creativecommons.org/licenses/by/4.0/>).

## 1. Introduction

The study of fatigue in metallic materials dates back to the 19th century and the pioneering research by Wöhler on failures in railroad rails [1].

Among the plethora of materials susceptible to fatigue, copper alloys have garnered considerable attention due to their widespread industrial usage and unique mechanical properties. Understanding the fatigue behavior of copper alloys is essential to enhance the reliability and durability of numerous engineering components that range from structural elements in the aerospace and automotive industries to electrical connectors and heat exchangers. S-N curves represent the relationship between the amplitude of applied stress (S) and the number of cycles to failure (N) for a given material, whereas  $\epsilon$ -N curves represent the relationship between the amplitude of applied strain ( $\epsilon$ ) and the number of cycles to failure (N). In heat transfer systems, such as pumps and heat exchangers, it is common to join various components by copper tubes that are subjected to temperature, pressure and vibration. These loads induce stresses in the tubes that can lead to system failure. Graphs that correlate stresses and strains to the number of cycles (S-N and  $\epsilon$ -N) enable engineers to determine safe design limits for stress and strain. Studies of pure copper have been conducted for projects that require extremely high reliability, such as nuclear power plants, synchrotrons or the ITER (International Thermonuclear Experimental Reactor) [2]. In addition, the development of high-power piezo-ceramic actuators since 1950 [3] has

enabled the reliable execution of high-cycle fatigue (HCF) and very high-cycle fatigue (VHCF) tests within a short timeframe and at high frequencies using the ultrasonic fatigue testing approach. Additionally, with the development of Equal Channel Angular Pressing (ECAP) processes since the 1970s [4], studies of fatigue resistance in materials like copper have been conducted, as their fatigue resistance at low cycles is improved by achieving ultrafine grain sizes. Although most fatigue studies focus on iron, aluminum and titanium alloys, the current review concentrates on high-purity copper (Cu-DHP) and some of its alloys of similar composition. The latter include electrolytic tough-pitch (ETP), oxygen-free electronic (OFE) and oxygen-free (OF). Despite the extensive research on copper properties, as well as its versatility and prevalent use in electrical and electronic applications, the use of copper under cyclic loads is relatively limited. The common use of copper in rotating machines for power generation is highlighted [5]. A challenge that is associated with copper is its embrittlement in the presence of hydrogen, especially when the former contains oxygen [6]. It is noted that phosphorus-deoxidized coppers, historically used in non-critical electrical conductivity applications such as tubes, present fewer challenges than copper in electrical or electronic applications. The review addresses a detailed compilation of data of Cu-DHP (phosphorus-deoxidized copper) and similar alloys that are provided for comparison. Various failures that are associated with these types of copper have been studied and are discussed in detail. They include the type of load and its frequency of application, temperature, chemical environment, grain size, metallurgical condition and load type. This presents a comprehensive understanding of their behavior under the cyclic loads for both high-cycle (HCF) and low-cycle fatigue (LCF). A thorough examination of HCF was carried out, and stress–life (S–N) curves were constructed to establish a relationship between the number of cycles before failure (N) and the stress amplitude ( $\sigma_a$ ) under conditions of zero mean stress ( $\sigma_m = 0$ ). Considering non-zero mean stress ( $\sigma_m \neq 0$ ), and based on the Gerber–Elliptic and Soderberg failure criteria, several stress–life (S–N) curves that correlate fatigue strength ( $S_e$ ) with stress amplitude ( $\sigma_a$ ), yield strength ( $S_{yp}$ ) and ultimate strength ( $S_{ut}$ ) were also determined. Finally, for LCF, strain–life ( $\epsilon$ –N) curves were formulated that establish a connection between the number of cycles before failure (N) and the total strain amplitude ( $\epsilon_{plastic}$ ). In turn, this provides valuable insights for future developments in the utilization of these materials.

## 2. Mechanical Fatigue Data Review

### 2.1. High-Cycle Fatigue: Stress–Life (S–N) Approach to Predict the Fatigue Damage

#### 2.1.1. Fatigue Strength ( $S_e$ ) and Zero Mean Stress ( $\sigma_m = 0$ )

Due to its extensive use in various industrial sectors, copper stands out as one of the most extensively studied metallic materials. A plethora of data are available for copper applications where electrical conductivity is paramount. These include electronic and electrical applications, where the copper purity is higher than that in heat pump tubes. However, there are limited references for Cu-DHP. This material has fewer references due to its application in contexts that require lower reliability. One of the earliest references is provided by the Deutsches Kupfer Institut [7]. Its fatigue strength ( $S_e$ ) data were published in the Copper Data Sheet A6 [8] for zero mean stress ( $\sigma_m = 0$ ), as depicted in Figure 1. The graph data in the foregoing figure pertain to 0.8 mm thick strips with 21%, 37% and 60% cold work (CW), as obtained from Burghoff [9]. Additionally, Hoyt [10] reported that for annealed Cu-DHP copper tubes with a grain size of 50  $\mu\text{m}$ , a limit of 75 MPa was established for  $20 \times 10^6$  cycles, and limits of 100 and 135 MPa were established for 15% and 40% cold work (CW), respectively. The results of both investigations can be observed in Table 1.

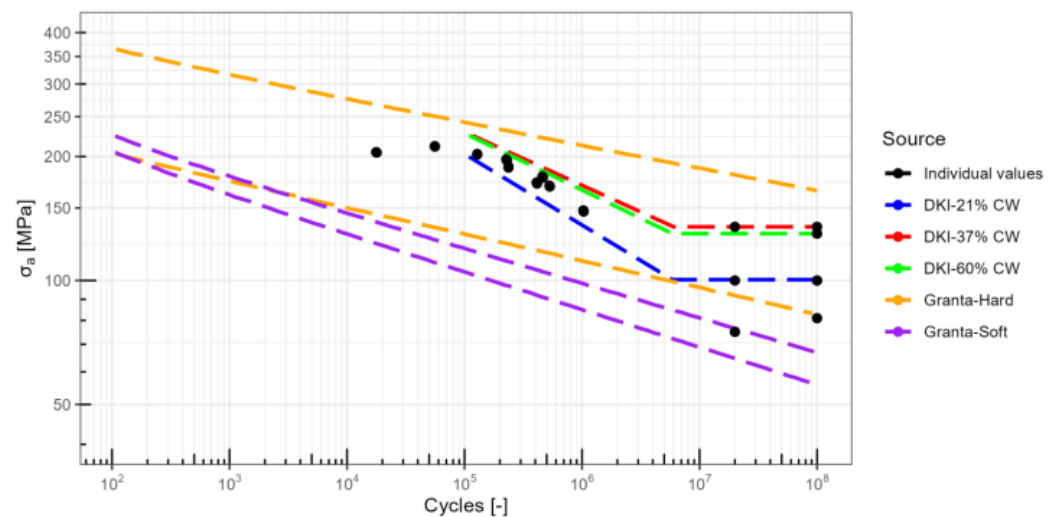


**Figure 1.** Fatigue strength ( $S_e$ ) data for Cu-DHP. Individual values correspond to pipe and strips of Cu-DHP annealed and cold-worked in several grades and tested in air at room temperature.

**Table 1.** Fatigue strength ( $S_e$ ) data from Copper Data Sheet A6 [8].

| Form              | Treatment                           | N° Cycles<br>[ $\times 10^6$ ] | Ultimate<br>Strength [MPa] | Fatigue<br>Strength $S_e$ [MPa] | Authors      |
|-------------------|-------------------------------------|--------------------------------|----------------------------|---------------------------------|--------------|
| Strip, Th. 0.8 mm | CW 21%                              | 100                            | 300                        | 100                             | Burghoff [9] |
| Strip, Th. 0.8 mm | CW 37%                              | 100                            | 360                        | 135                             | Burghoff [9] |
| Strip, Thh 0.8 mm | CW 60%                              | 100                            | 415                        | 130                             | Burghoff [9] |
| Pipe              | Annealed.<br>Grain size<br>0.050 mm | 20                             | 225                        | 75                              | Hoyt [10]    |
| Pipe              | CW 15%                              | 20                             | 280                        | 100                             | Hoyt [10]    |
| Pipe              | CW 40%                              | 20                             | 385                        | 135                             | Hoyt [10]    |

The copper alloy manufacturing company Wieland [11] provides an estimate ( $S_e$ ) of one-third of the tensile strength ( $R_m$ ) for  $10^7$  cycles. For instance, the fatigue strength ( $S_e$ ) of Cu-DHP with  $R_m = 210$  MPa is estimated to be 70 MPa. Additional  $S_e$  data are available from databases such as Granta [12] and measurements conducted by Park et al. [13]. The limited data for the  $S_e$  of Cu-DHP are illustrated in Figure 1.

Due to the limited data available for Cu-DHP, one approach to estimate its fatigue behavior was to compare it to alloys that have a significantly high copper content. As indicated in Table 2, the differences in chemical composition between electrolytic tough-pitch (ETP), oxygen-free electronic (OFE), oxygen-free (OF) and deoxidized oxygen-free (DHP) are minimal, as all alloys involve a minimum of 99.90% Cu.

**Table 2.** Different types of high-purity coppers.

| Designation | Type of Copper                               | UNS    | Cu [%] |
|-------------|--|--------|--------|
| ETP         | Electrolytic tough-pitch (ETP)               | C11000 | 99.99  |
| OFE         | Oxygen-free electronic (OFE)                 | C10100 | 99.95  |
| OF          | Oxygen-free (OF)                             | C10200 | 99.90  |
| DHP         | Phosphorized, high-residual phosphorus (DHP) | C12200 | 99.90  |

A comprehensive analysis of fatigue properties for copper, specifically ETP and OF, can be found in Murphy [14], where data for factors such as the loading type, frequency, grain size or temperature are compiled. The effects of these factors on fatigue are shown in Figures 2–9.

### Stress Type Factor

For example, Figure 2 shows the effect of the load type on the fatigue strength ( $S_e$ ) of copper of high purity when considering push-pull (PP) and reverse bending (RB) loads. The results suggest that the lowest values of fatigue strength ( $S_e$ ) are obtained under the tensile loads. These are in agreement with observations relating to steel materials [15,16]. The numerical data that were available originally in graphical form only were extracted from the Murphy [14] experiments by WebPlotDigitalizer software (<https://automeris.io/WebPlotDigitizer.html>, accessed on: 4 December 2023) [17]. The regression equations were determined for these data by Rstudio 2023.09.1 software [18] and R 4.3.2 [19]. In this case, log-log linear regression equations (stress–life (S-N) curves) were determined for the relationship between stress amplitude ( $\sigma_a$ ) and the number cycles to failure (N) for PP and RB loads (See Figure 2).

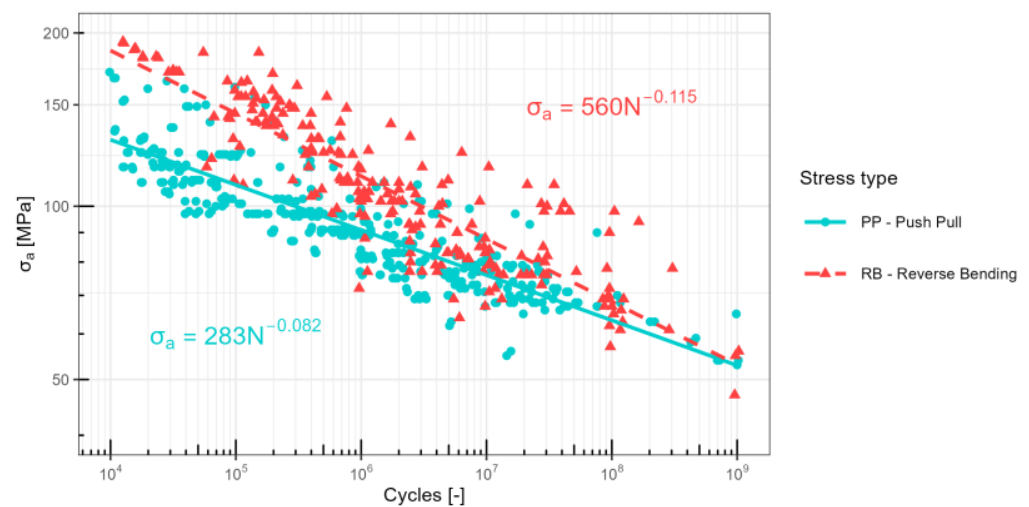


**Figure 2.** Effect of load type on the fatigue strength ( $S_e$ ) of copper of high purity Reprinted with permission from ref. [14] John Wiley & Sons 1985. Tests of smooth bars conducted in air at room temperature under zero mean stress conditions ( $R = -1$ ).

### Frequency Factor

In regard to Murphy's data, the frequency between 0.1 and 150 Hz does not exhibit as significant an effect as the loading type (Figure 3). In recent years, there has been an increased interest in the effects of frequency on the fatigue strength ( $S_e$ ) of metals due to the emergence of high-frequency testing machines. The frequency effect has been studied in various metals, including polycrystalline copper. A comprehensive summary is available in Tahmasbi et al. [20]. These authors emphasize that fatigue properties change, as high-load ultrasonic tests produce different failure modes than conventional tests. Other authors, such as Marti et al. [21], found no significant difference between tests at 20 and 100 Hz. However, they observed differences at high frequencies. Thus, they concluded that the fatigue mechanism changes at high frequencies: "This frequency effect was attributed to two key time-dependent mechanisms in persistent slip band formation and extrusion growth: cross slip of screw dislocations and production/diffusion of vacancies." Fintová et al. [22] also noted an increase in fatigue strength ( $S_e$ ) between 80 and 20 kHz. Similar results were found by Stanzl-Tschegg [23] and Phung [24]. A comparative summary of values at low and high frequencies that the aforementioned researchers obtained can be seen in Figure 4. It is noteworthy that the lowest fatigue strength ( $S_e$ ) values that were reported by these authors and Singh et al. [25] were obtained at a very low frequency of 0.5 Hz. As for Figure 2, the relationship between  $\sigma_a$  and N was determined in Figures 3 and 4 for each of the data sets depending on the frequency of the load applied in the fatigue test. It should be noted that the data at ultra-high-cycle fatigue (UHCF) do not describe a straight line in the log-log plot.

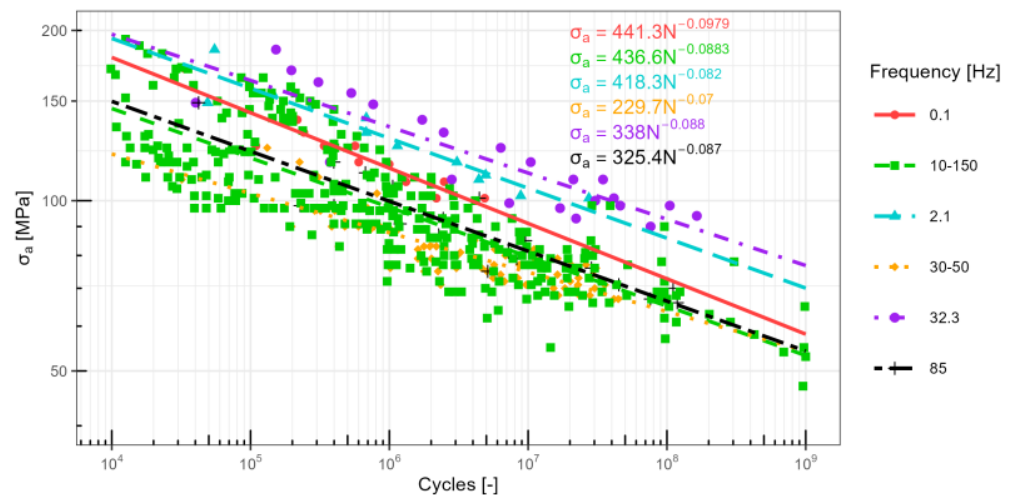


**Figure 3.** Effect of frequency on the fatigue strength ( $S_e$ ) of copper of high purity reprinted with permission from ref. [14] John Wiley & Sons 1985. Testing was conducted in air at room temperature in zero mean stress conditions ( $R = -1$ ), material TP or OF, reverse bending and push-pull, 0.1, 2.1 and 32.3 Hz cold-worked, 30–50, 85 and 10–150 Hz annealed. 30–50 Hz in several environments: lab air, vacuum, damp nitrogen, damp pure air and dry pure air.

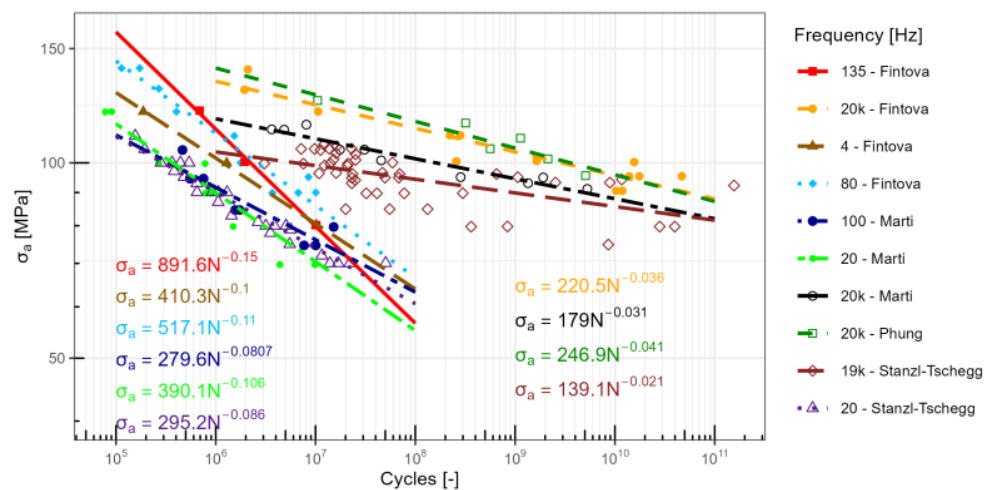


**Figure 4.** Reference data by frequency (reprinted with permission from refs. [21–24] Elsevier Science & Technology Journals 1988, 1996, 1979). Test conditions: Fintova: cold-rolled ETP in air at room temperature, push-pull. Marti: OFHC in air at room temperature, push-pull. Stanzl-Tschegg: ETP 99.98 and ETP in air at room temperature, push-pull. Phung: strengthened OFHC in air at room temperature, push-pull.

It appears that whether fatigue testing is controlled by strain or by stress has no significant effect, as noted by Singh et al. [25]. Those authors also suggested that radiation may have a slightly beneficial effect on fatigue duration.

#### Grain Size Factor

With regard to the grain size effect on copper fatigue strength ( $S_e$ ), improvements in resistance are observed for cycles below  $10^6$  (Figure 5). This is not distinctly evident in Murphy's data [14]. Numerous authors [26–36] have compared ultrafine grain sizes achieved by “Equal-Channel Angular Pressing (ECAP)” to grain sizes that are more typical in the industry (Figure 6). Li et al. [30] reached similar conclusions as previous studies but added that fatigue strength ( $S_e$ ) in torsion improves with ultrafine grain (UFG). The relationship between  $\sigma_a$  and  $N$  was also calculated for each data set according to the grain

size in both figures. Fatigue in coarse-grain copper is correlated with deformation, which is characterized by frequent cross-slip events [37]. For UFG copper grain refinement and work hardening, the increase in the average dislocation density has an important role in determining the resulting properties [35].

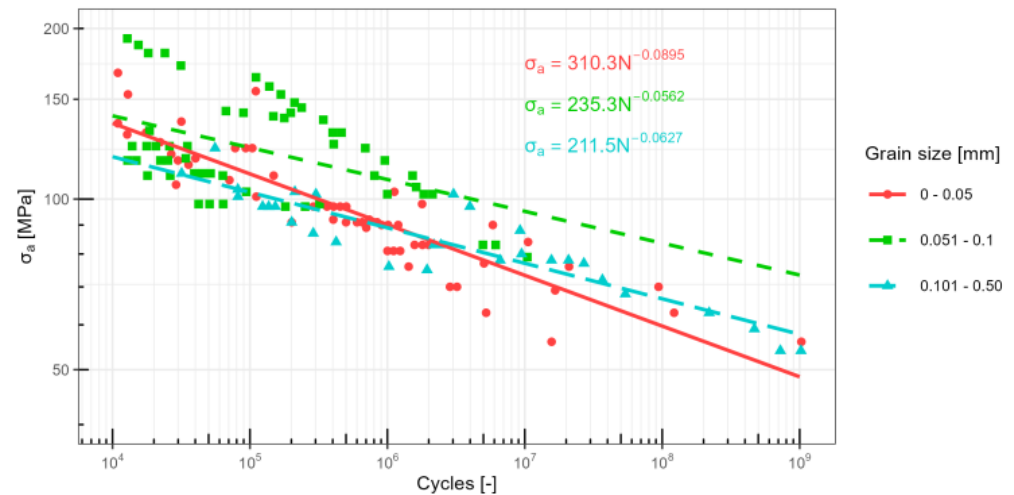


**Figure 5.** Effect of grain size on the fatigue strength ( $S_e$ ) of high-purity copper reprinted with permission from ref. [14] John Wiley & Sons 1985. Test conditions. 0–0.05: Annealed TP or OF, in air at room temperature, reverse bending and push-pull. 0.051–0.1: Annealed TP or OF, in air at room temperature, reverse bending and push-pull. 0.101–0.50: Annealed TP or OF, in air at room temperature, push-pull.

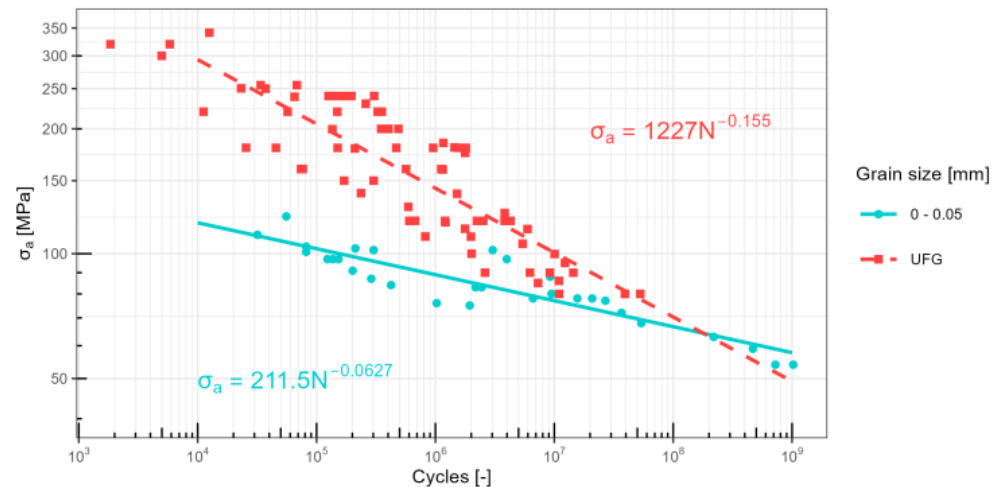


**Figure 6.** Effect of grain size on the fatigue strength ( $S_e$ ) of high-purity copper. (UFG: ultrafine grained.) Test conditions. 0–0.05: Annealed TP or OF, in air at room temperature, reverse bending and push-pull. UFG: OF, in air at room temperature, reverse bending, torsion and push-pull.

#### Cold Work Level Factor

The data published by Murphy [14] for different levels of cold work (Figure 7) suggest that the more cold work that is applied, the higher the fatigue strength ( $S_e$ ). This agrees with more recent references on copper subjected to Equal-Channel Angular Pressing (ECAP) [26,28,31,32,35,36]. This figure also shows the relationship between  $\sigma_a$  and  $N$  for each data set based on the metallurgical state.

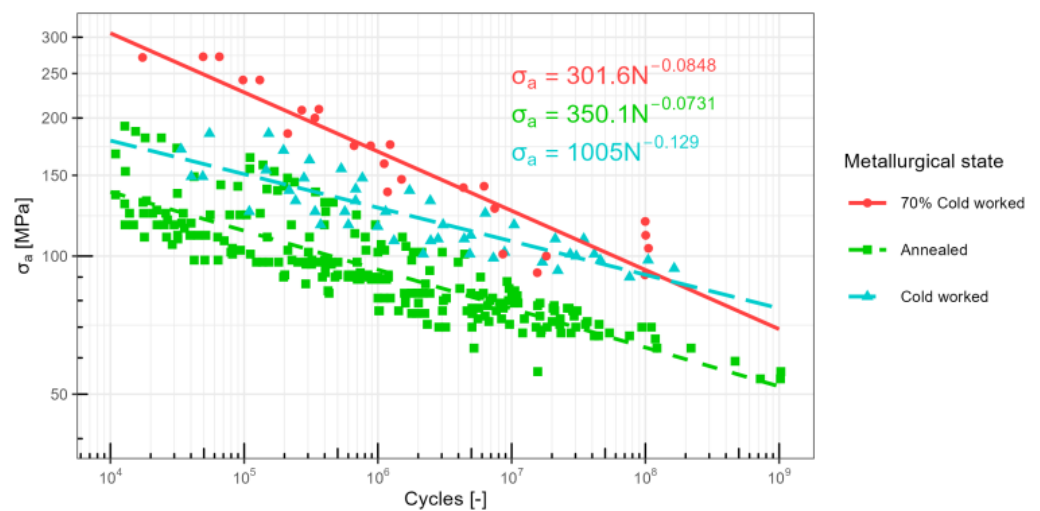


**Figure 7.** Effect of metallurgical condition on the fatigue strength ( $S_e$ ) of copper of high purity reprinted with permission from ref. [14] John Wiley & Sons 1985. Test conditions. 70% cold-worked: Cold-worked 70% OF or TP, in air at room temperature. Annealed: Annealed TP or OF, mainly in air, a few in damp nitrogen at room temperature, reverse bending and push-pull, several frequencies. Cold-worked: Cold-worked TP or OF in air at room temperature, reverse bending and push-pull and several frequencies.

#### Environment Factor

Additionally, some researchers have studied how the fatigue strength ( $S_e$ ) of copper of high purity is influenced by the chemical environment in which the copper materials operate. It appears that there is some improvement when working in a vacuum (Figure 8). In this context, Thomson et al. [38] determined that the fatigue strength ( $S_e$ ) can be increased by preventing access to oxygen on the surfaces. Duquette [39] concluded that oxygen and water vapor reduce fatigue life, whereas Mughrabi [40] observed a longer life in a vacuum than in air. Similarly, Wang et al. [41] found that compared to air, a vacuum produced significant improvements in fatigue life for high-purity copper. Figure 8 indicates the relationship between  $\sigma_a$  and  $N$  for each data set, taking the environment into account.

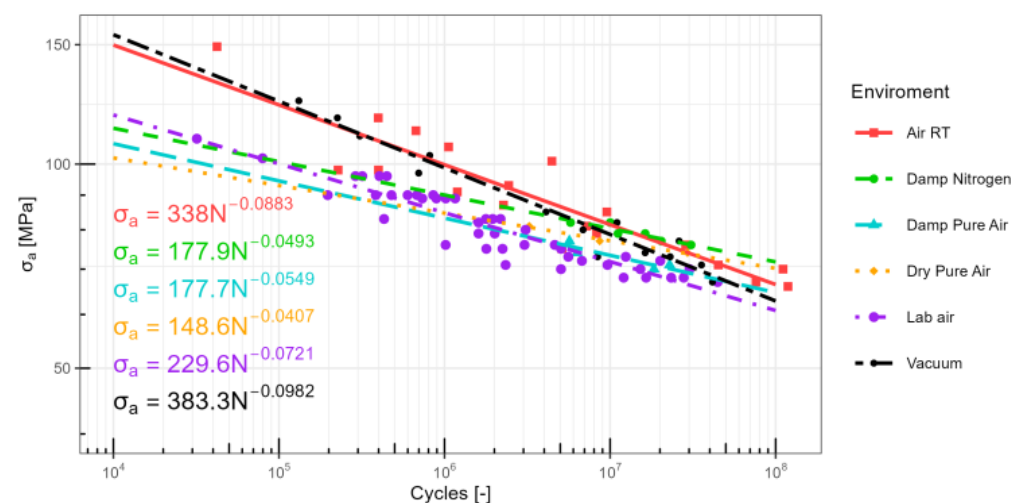


**Figure 8.** Fatigue strength ( $S_e$ ) data categorized by environment. Murphy reprinted from Ref. [11]. Test conditions. Air RT: Annealed TP in air at room temperature, reverse bending and push-pull, 85 Hz. Damp nitrogen: Annealed TP or OF at room temperature, push-pull, 30–50 Hz. Damp pure air: Annealed TP or OF at room temperature, push-pull, 30–50 Hz. Lab air: Annealed TP or OF at room temperature, push-pull, 30–50 Hz. Vacuum: Annealed TP or OF at room temperature, push-pull, 30–50 Hz.

### Temperature Factor

In addition, other authors, including Simon et al. [42], studied the effect of temperature on the fatigue strength ( $S_e$ ) of Cu-OF (Figure 9). The results have shown that the lower the test temperature, the greater the fatigue strength ( $S_e$ ). The relationship between  $\sigma_a$  and  $N$  for each data set, categorized by the temperature, is also illustrated in Figure 9.

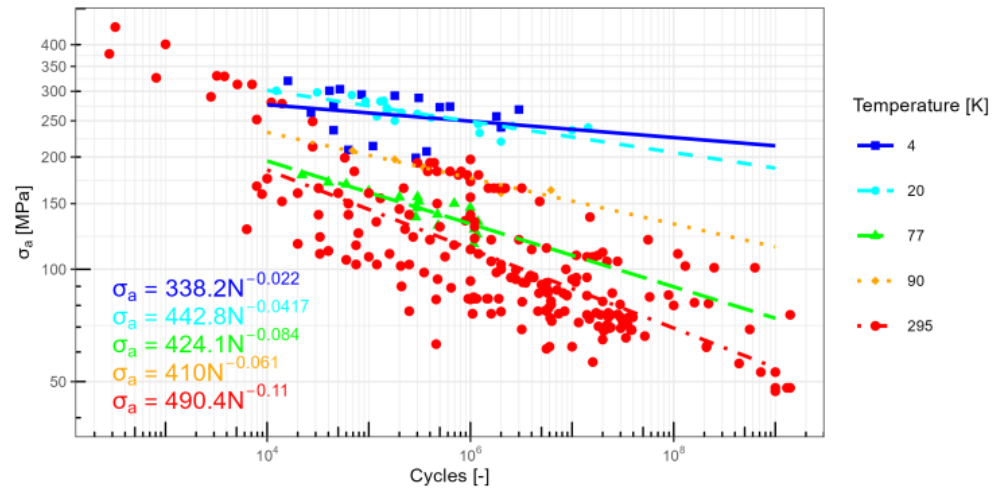


**Figure 9.** Fatigue strength ( $S_e$ ) data categorized by temperature (Simon reprinted from Ref. [42]). Test condition. 4: Annealed OF in air/liquid, push-pull. 20: Annealed OF in air/liquid, push-pull. 77: Annealed OF in air/liquid/vacuum/liquid nitrogen, push-pull. 90: Annealed OF in air/liquid, push-pull. 295: Annealed OF in air/liquid/vacuum/liquid nitrogen/dry purified air/damp purified air, push-pull.

### Material Factor

Additionally, Murphy [14] analyzed several types of materials, such as OF and ETP, and found no significant difference in their fatigue strengths (Figure 10). This suggests that similar results could be expected for Cu-DHP. The relationship between  $\sigma_a$  and  $N$  for each data set, categorized by the type of pure copper, is also illustrated in this figure.

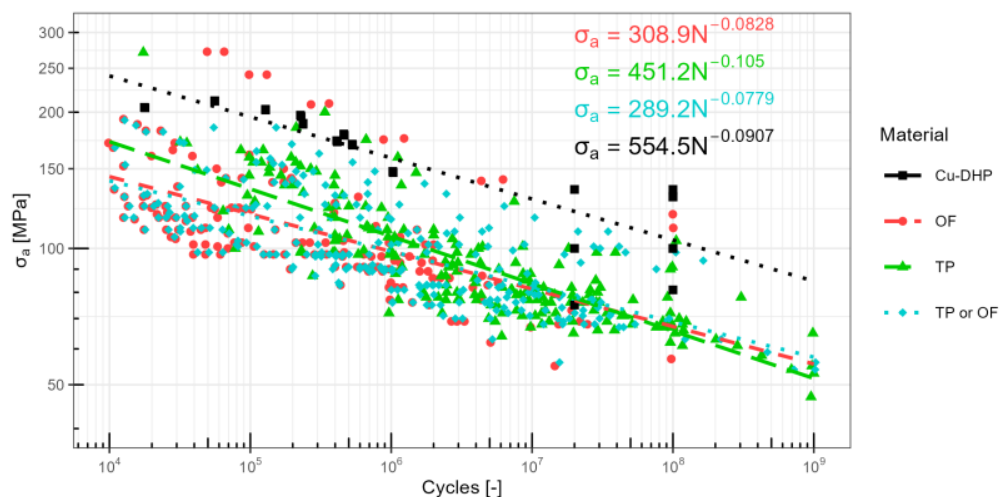


**Figure 10.** Fatigue strength ( $S_e$ ) data categorized by type of pure copper (Murphy reprinted with permission from ref. [14] John Wiley & Sons 1985). Test conditions. Cu-DHP: Cu-DHP at different metallurgical states, in air at room temperature, reverse bending and push-pull. OF: OF at several metallurgical states in air at room temperature, push-pull and reverse bending, 10–150 Hz.

Figures 11 and 12 illustrate the fatigue strength ( $S_e$ ) of Cu-DHP when it is compared to that obtained for other copper grades. This figure shows how the Cu-DHP data would

fall within the scatter plot. The figure also indicates more variation in the tested parameters for higher-purity coppers than for Cu-DHP. In the absence of more Cu-DHP data, these findings could be used as fatigue limits, considering the various variants.

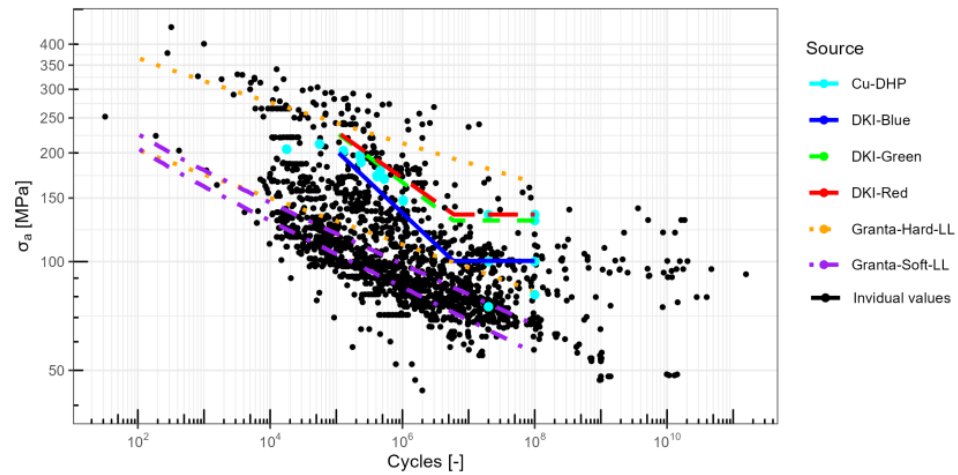


**Figure 11.** Fatigue strength ( $S_e$ ) data of ETP, OFE, OF and Cu-DHP.

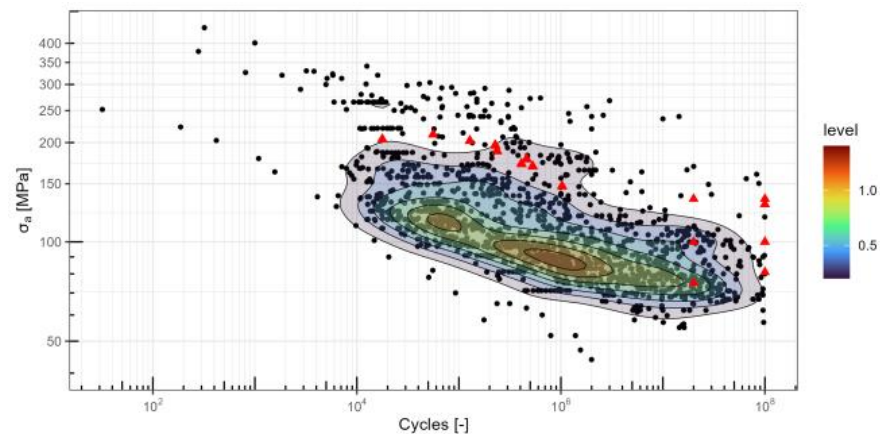


**Figure 12.** Fatigue strength ( $S_e$ ) data of ETP, OFE, OF and Cu-DHP compiled according to the corresponding authors. Cu-DHP data are depicted using red triangles, while other copper samples are represented by black dots.

### 2.1.2. Fatigue Strength ( $S_e$ ) and Non-Zero Mean Stress ( $\sigma_m \neq 0$ )

As in the case of fatigue data with zero mean stress, finding references for the non-zero mean stresses is challenging. However, this was resolved by taking advantage of the data collected for copper by Murphy [14] and considering mean and alternating stresses for copper. The Gerber [43] and Soderberg [44] failure criteria are provided in the Haigh diagram [45] in Figures 13 and 14. For  $10^7$  cycles, a combination of Gerber, Soderberg and ASME elliptic criteria has been modified by multiplying the endurance limit (Equation (1)) by 0.75 and by 0.68 for  $10^8$  cycles (Equation (2)).

$$\left( \frac{\sigma_a}{0.75 \cdot S_{e(10^7)}} \right)^2 + \left( \frac{\sigma_m}{S_{ut}} \right)^2 = 1 \quad (1)$$

$$\left( \frac{\sigma_a}{0.68 \cdot S_{e(10^8)}} \right)^2 + \left( \frac{\sigma_m}{S_{ut}} \right)^2 = 1 \quad (2)$$

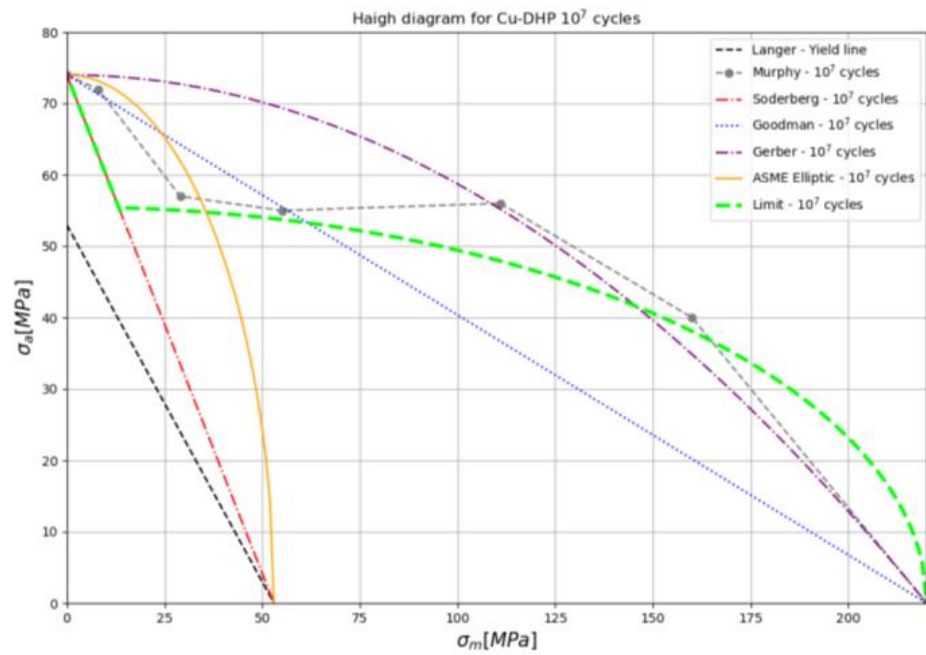


**Figure 13.** Haigh diagram with Murphy data and a proposed limit of 10<sup>7</sup> cycles. Test carried out on OF in air at room temperature at 85 Hz, push-pull under different mean stress conditions.

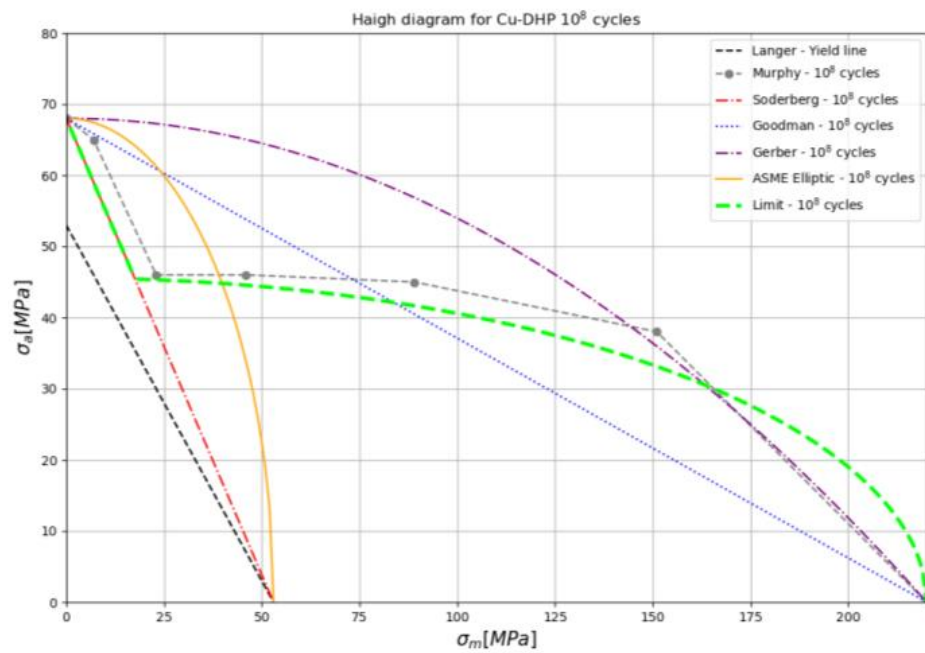


**Figure 14.** Haigh diagram with Murphy data and a proposed limit of 10<sup>8</sup> cycles. Test conducted on OF, in air at room temperature at 85 Hz, push-pull under different mean stress conditions.

In the case of the Soderberg criterion, Equations (3) and (4) are used in the low range of the mean stress to define limits of 10<sup>7</sup> and 10<sup>8</sup> cycles, respectively.

$$\frac{\sigma_a}{S_{e(10^7)}} + \frac{\sigma_m}{S_{yp}} = 1 \tag{3}$$

$$\frac{\sigma_a}{S_{e(10^8)}} + \frac{\sigma_m}{S_{yp}} = 1 \tag{4}$$

## 2.2. Low Cycle Fatigue (LCF): Strain–Life ( $\epsilon$ - $N$ ) Approach to Predict the Fatigue Damage

Very few researchers apart from Tamiya [46] and Harun et al. [47] have studied low-cycle fatigue of Cu-DHP. Thus, for example, Tamiya [46] subjected CU-DHP tubes to a fatigue load by varying the internal pressure. This research concludes that the fatigue life in bent tubes with internal pressure variations can be estimated with the plastic deformation calculated by elastic stresses and corrected with Neuber's law [48]. Secondly, Harun et al. [47] reviewed different methods for estimating fatigue life and compared them to experimental data on cylindrical specimens that are subjected to tension-compression loads.

### Strain Data

A summary of the deformation data found for Cu-DHP and similar copper alloys appears below. The data that were analyzed for different alloys indicate that the low-cycle strength fatigue values are very similar (Figure 14) to those for OFHC and OF insofar as they can reach a maximum plastic strain amplitude ( $\epsilon_{plastic}$ ).

The data in Figure 15, which are grouped according to their corresponding copper alloy and their author, are shown in Figure 16.

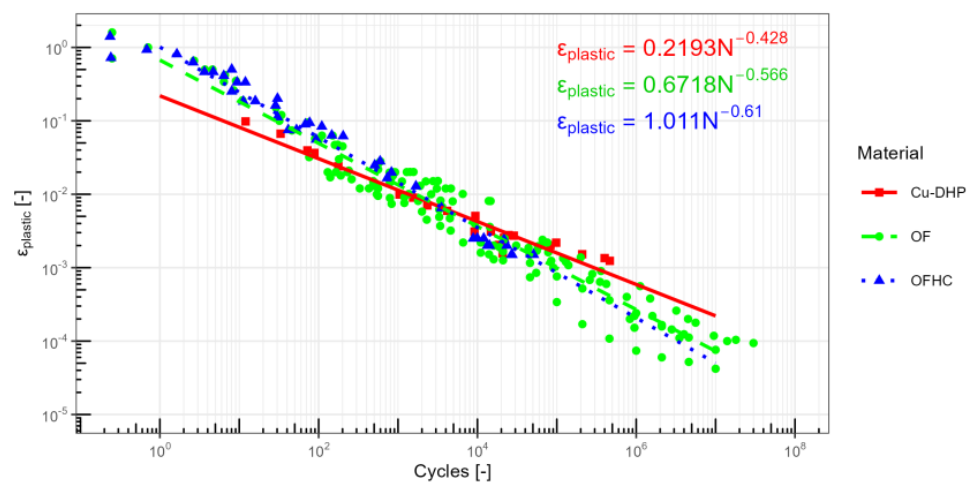


**Figure 15.** Plastic strain amplitude ( $\epsilon_{plastic}$ ) vs. number of cycles ( $N$ ) to failure of Cu-DHP, OF and OFHC. Test conditions. Cu-DHP: Cu-DHP in air at room temperature, push-pull. OF: Annealed OF in air/vacuum at room temperature, push-pull, several frequencies and temperatures. OFHC: Annealed OFHC in air at room temperature, push-pull, 0.5 Hz.

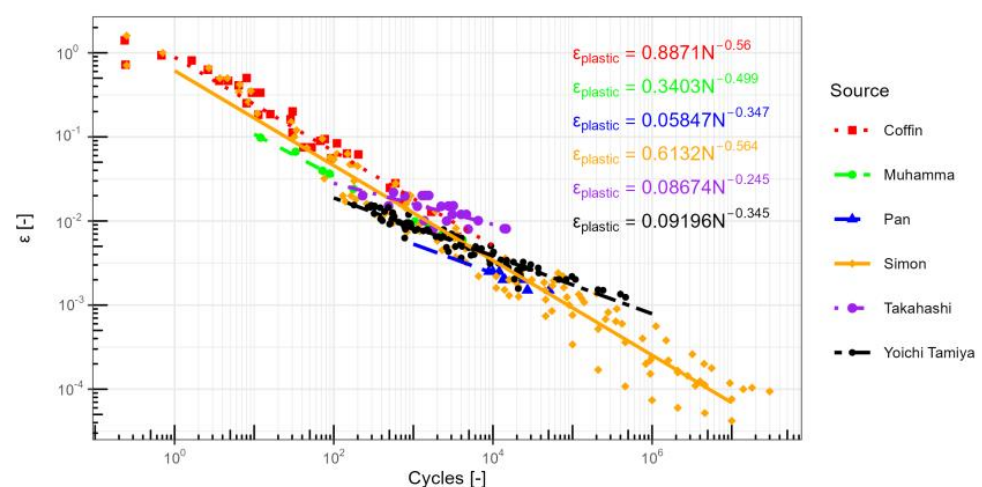


**Figure 16.** Plastic strain amplitude ( $\epsilon_{plastic}$ ) vs. number of cycles ( $N$ ) to failure according to different authors. Test conditions: Coffin: OFHC in air at room temperature. Muhamma: Cu-DHP in air at room

temperature, push-pull. Par: Annealed OFHC in air at room temperature, push-pull, 0.5 Hz. Simon: Annealed OF in air at room temperature, push-pull, several frequencies. Takahashi: OF at several temperatures in vacuum. Yoichi Tamiya: Cu-DHP and other coppers in air at room temperature.

Pan et al. [49] concluded for OFHC that the occurrence of fatigue depends largely on the grain size. They believe that the larger the grain size, the earlier the onset of the fatigue for a fixed plastic strain amplitude. One of the first relationships ( $\epsilon$ - $N$  curve) to fall between the plastic strain amplitude ( $\epsilon_{plastic}$ ) and the number of cycles ( $N$ ) is obtained from Figure 17. It was determined by Coffin [50] for OFHC copper:

$$\epsilon_{plastic} = 0.90(N)^{-0.502}. \quad (5)$$

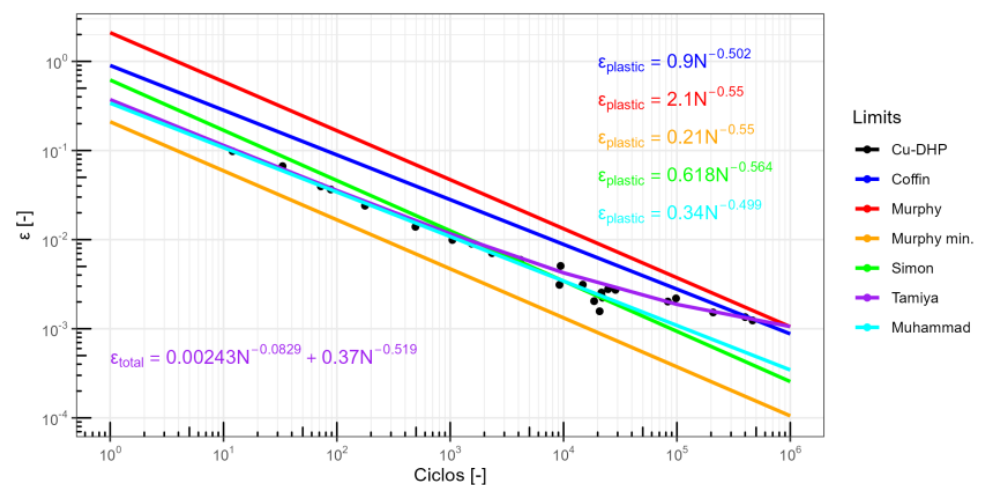


**Figure 17.** Plastic strain amplitude ( $\epsilon_{plastic}$ ) vs. number of cycles ( $N$ ) to failure of Cu-DHP with different adjustment lines. Test conditions described in previous figures.

Other authors, including Murphy [14], have proposed other coefficients between  $\epsilon_{plastic}$  and  $N$  for OF copper, considering the minimum values (see the line Murphy min.) that can be seen in Equation (6):

$$\epsilon_{plastic} = 0.21 \cdot N^{-0.55}. \quad (6)$$

In addition, for OF, Simon et al. [42] obtained the following coefficients between  $\epsilon_p$  and  $N$ :

$$\epsilon_{plastic} = 0.618 \cdot N^{-0.564}. \quad (7)$$

Finally, Tamiya [46] and other authors proposed other coefficients (Equation (8)) between the total strain amplitude ( $\epsilon_{Total}$ ) and  $N$  for Cu-DHP that combine the elastic ( $\epsilon_{elastic}$ ) and plastic strain ( $\epsilon_{plastic}$ ):

$$\epsilon_{Total} = \epsilon_{elastic} + \epsilon_{plastic} = 0.00243 \cdot N^{-0.0829} + 0.37 \cdot N^{-0.519}. \quad (8)$$

It has been observed that the data obtained by Harun et al. [47] fit well with Equation (8). This was proposed by Tamiya [46] and can be seen in Figure 17. However, the relationships between the  $\epsilon_{plastic}$  and  $N$  obtained by Harun et al. [47] can be expressed as:

$$\epsilon_{plastic} = 0.34 \cdot N^{-0.499} \quad (9)$$

Finally, for the effect of temperature, it has been observed that the low-cycle fatigue strength ( $S_e$ ) generally decreases as the temperature increases in a vacuum. However, Takahashi et al. [51] concluded that there are no significant differences in low-cycle fatigue strength ( $S_e$ ) between 100 and 300 °C in a vacuum (see Figure 18).

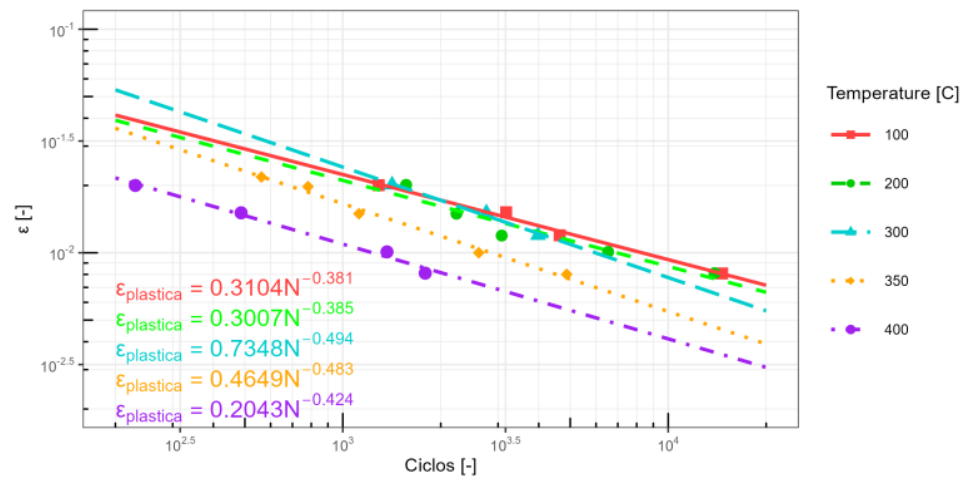


**Figure 18.** Plastic strain amplitude ( $\epsilon_{plastic}$ ) vs. number of cycles ( $N$ ) to failure: the effect of temperature on fatigue strength ( $S_e$ ) at a low number of cycles reprinted from Ref. [51]. Test conditions, OF in vacuum at several temperatures.

### 3. Other Factors

For the fatigue analysis of copper tubes, special attention must be paid to bent areas and welded joints. Residual stresses accumulate in bent areas from the bending of the tube. Depending on the type of stress, bi-axiality states can also occur, which can contribute to premature failure.

#### 3.1. Brazing Zone

##### 3.1.1. Heat-Affected Zone

As previously mentioned, grain size significantly influences fatigue strength. Improper brazing can adversely affect grain size and, consequently, fatigue strength. It is imperative to consider the various grades of copper applicable to the heat pump. The copper tubes, which link components such as the compressor and heat exchangers, exhibit a smaller and more controlled grain size. Conversely, the connector used for welding to these tubes, notably larger in diameter, features a larger grain size (see Figures 19 and 20). Particularly at low cycle counts, larger grain sizes correlate with lower fatigue strength. Figures 19 and 20 do not indicate a direct impact of brazing on grain size, yet a noticeable discrepancy exists between the grain sizes of the tube and heat exchanger connector. According to Zhibi Wang [40], the brazing process can reduce yield strength by 30 to 40 MPa, potentially affecting fatigue life. This effect is evident in the Haigh diagram, where certain failure criteria are contingent upon yield strength.

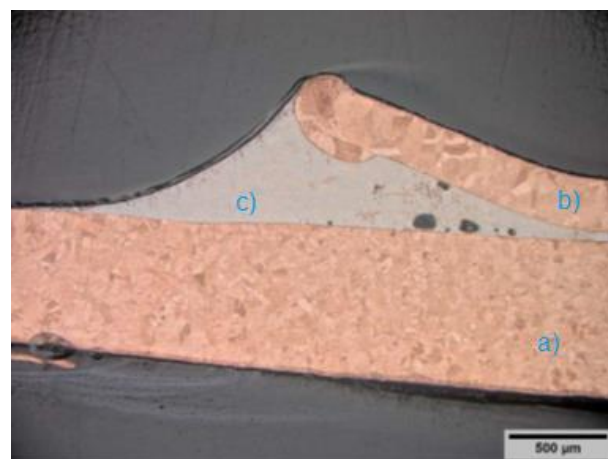


**Figure 19.** Optical microscopy image depicting a longitudinal cross-section of a copper-copper brazing joint. (a) Cu-DHP with average grain size 16–60 mm, (b) Cu-DHP with coarse grain size, (c) brazing material.



**Figure 20.** Optical microscopy image depicting a longitudinal cross-section of a copper-copper brazing joint. (a) Cu-DHP with averaged grain size 16–60 mm, (b) Cu-DHP with coarse grain size, (c) brazing material.

### 3.1.2. Liquid Metal Embrittlement

Another failure mode that could be encountered near the weld is that of liquid metal embrittlement. Copper is susceptible to embrittlement by Hg, Ga, Zn, Sn, Pb, Bi, Li, Na and In [52–55].

### 3.1.3. Stress Concentration

In addition, this zone could be thermally affected by brazing and a slight change in thickness. For example, a drop of brazing material could induce a concentration of stress and a breakage at a lower number of cycles.

## 3.2. Bent Tubes and Field Failures

Several studies related to Cu-DHP [56–58] concentrate failures in air-conditioning applications. Cu-DHP is a material that is commonly used for heat exchangers and for the tubes that connect them to the other components. These tubes are mechanically bent to produce the desired geometry. They undergo plastic deformation in this process and leave a zone of residual stress accumulation. This, together with a notch, ammonia residues and/or mechanical loads, appears to be the cause of the failures. The residual stress accumulation zone is a constant in several failures that are associated with Cu-DHP pipes. Park [13] conducted a fatigue analysis of bent copper tubes of differing bend radii. McDougal and Stevenson [57] analyzed another failure in a U-shaped tube that was due to SCC (Stress Corrosion Cracking) and also fostered by residual stresses and the presence of residual ammonia from production processes. Examples of cracks in bend copper pipes can be seen in Figures 21 and 22.



**Figure 21.** Photo of the copper tube failure studied by McDougal and Stevenson reprinted with permission from ref. [57] Springer Nature BV, 2004.



**Figure 22.** Photo of the copper tube failure studied by Stevenson reprinted with permission from ref. [58] Springer Nature BV, 2004.

Stevenson [58] analyzed the failure of a U-bent tube and concluded that the fatigue failure had been promoted by residual stresses.

Duffner [56] discusses a failure in a straight zone, but the author also related it to SCC, residual stresses and surface defects. Pantazopoulos [59] analyzed a failure in an air-conditioning application. This failure appeared in a bent section of pipe. He concluded that the failure was caused by mechanical fatigue that was initiated on the outside of the pipe. The same author also analyzed another failure [60] in the same area and concluded that it was caused by mechanical fatigue on the inside of the tube, together with the accumulation of residual stresses. A very comprehensive analysis of the failure of a Cu-DHP elbow in a heat exchanger is documented by Miyamoto [61]. This elbow is not subjected to mechanical loads, apart from pressure and temperature variations. Instead, it failed due to IGSCC (Inter-Granular Stress Corrosion Cracking) as a result of the accumulation of residual stresses. Kim [62,63] conducted an analysis of residual stress distribution in the bent area of the pipe. He undertook a finite element simulation of the residual stress distribution and validated it by Raman spectroscopy. A low-cycle fatigue SEM can be seen in Figure 23.

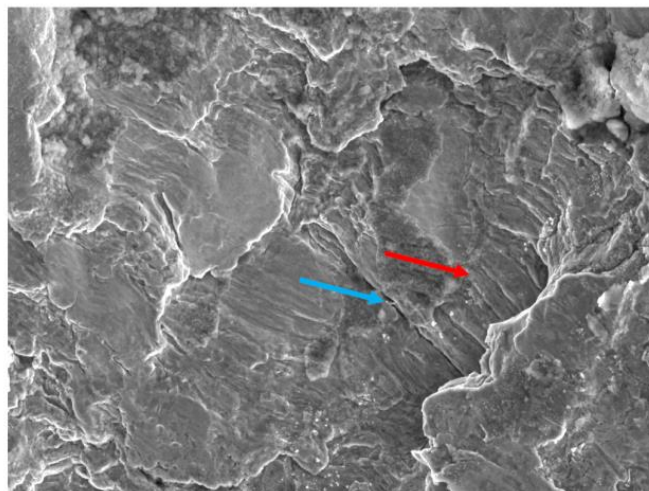


**Figure 23.** Low-cycle fatigue failure in a Cu-DHP tube. Red and blue arrows show stretch marks from fatigue.

#### 4. Discussion

One of the main objectives of this study was to compile available data in the literature regarding fatigue of Cu-DHP. As data for this material are very limited, the data collection has been extended to coppers of very similar composition.

A collection of fatigue data covering the variability of factors analyzed in this meta-analysis has been obtained. Figure 12 is an example of this. In Figures 10–12, the few data

points available for Cu-DHP have been plotted. Compared to the other materials, these data points are located at the upper end of the point cloud.

Due to the limited data and different factors analyzed in Cu-DHP, the lower line described by the data cloud should be considered for the purpose of caution. However, ultimately, this depends on the analyst and the reliability that the final application requires. The  $\epsilon$ -N curve for Cu-DHP demonstrates superior performance beyond  $10^6$  cycles compared to other copper alloys, but at the same time, it presents worse behavior at low cycles.

Although regression lines have been calculated for the different values of the factors, it must be emphasized that these data, which originated in a meta-analysis, are not well balanced, as in a designed experiment. However, they serve as a reference for understanding how the different factors affect fatigue. A study elucidating statistical models of copper fatigue can be found in Harlow [64], although its scope is confined to annealed electrolytic copper wire tested in reverse torsion fatigue.

The type of loading seems to affect copper similarly to steel. However, for copper, the tension-compression behavior is more demanding than flexion, although the effects for copper are equal beyond a certain number of cycles.

The loading frequency has little effect between frequencies from 0 to 300 Hz. However, the lowest values are obtained with the lowest analyzed frequency. This fact could be related to the increased exposure of the tested specimen to the surrounding atmosphere. This could promote oxidation negatively, thereby affecting the results.

It should be noted that there is a significant difference in behavior between the aforementioned frequencies and frequencies of the order of 20 kHz, as seen in Figure 4. Also, the values of frequencies that are of the order of 20 kHz do not describe a straight line in a log-log graph. Regression lines have been calculated to highlight the different behaviors.

Grain size is another factor that produces a significant variation in fatigue strength at low cycles. However, once a cycle threshold is exceeded, this strength equals approximately  $10^7$ – $10^8$  cycles (Figures 5 and 6). The effect of the level of cold work is similar to that attributable to grain size, with higher levels of work resulting in better fatigue resistance and smaller grain sizes expected in copper with more cold work (Figure 7). For low-cycle fatigue, Tanaka et al. [65] describes the effect of grain growth and the relaxation of strain.

In Figure 8, the effects of the surrounding atmosphere cannot be discerned due to the imbalance of this meta-analysis. However, several authors report an improvement in vacuum and avoid contact with oxygen.

In Figure 9, a clear improvement in resistance at low temperatures is evident. The effect of temperature can be seen on  $\epsilon$ -N curves at higher temperatures in the figure. Beginning at 300 °C, a reduction in fatigue resistance can be seen. This is consistent with the findings by Murphy [14].

Regarding the suggested failure criterion, it is worth mentioning that a visual modification has been implemented on the suggested formulas to position the fatigue failure points over the line we suggest. This signifies that the proposed criterion is more cautious in its prediction of failure, as it anticipates failure at cycles lower than the measured points. This criterion must be used with caution, as there are very few data points with mean stresses.

Attention must be given in the design of copper components to thermally affected areas, such as brazed zones and areas with residual stresses. The latter include curves that, in combination with the surrounding atmosphere, may lead to premature failure, as previously discussed.

## 5. Conclusions

In this article, a systematic literature review of the fatigue phenomenon in high-purity copper (Cu-DHP) and similar composition copper alloys has been conducted. The latter included electrolytic tough-pitch (ETP), oxygen-free electronic (OFE) and oxygen-free (OF) commercially pure copper metals (DHP, ETP, OF). All existing data have been compiled and plotted graphically by WebPlotDigitalizer and R software. The effect of different factors related to the fatigue strength ( $S_e$ ), such as the stress type, frequency, temperature, grain size, cold deformation and deformation amplitude, has been examined. With the data collected, stress–life (S-N) curves under zero mean stress ( $\sigma_m = 0$ ) were proposed for

high-cycle fatigue (HCF). Stress–life (S-N) curves were also established to correlate fatigue strength ( $S_e$ ), stress amplitude ( $\sigma_a$ ), yield strength ( $S_{yp}$ ) and ultimate strength ( $S_{ut}$ ) for non-zero mean stress ( $\sigma_m \neq 0$ ). These were based on a combination of Gerber, Soderberg and ASME elliptic failure criteria. For low-cycle fatigue (LCF), strain–life ( $\epsilon$ -N) curves were also developed that relate the number of cycles until failure (N) to the stress amplitude ( $\sigma_a$ ) and the total strain amplitude ( $\epsilon_{\text{plastic}}$ ). The analysis of the collected data enabled the formation of the following partial conclusions regarding the effect of various factors on the fatigue phenomenon:

- The effect of loading is more severe in the case of axial loading (tension-compression) than bending. The higher the number of cycles, the smaller the difference.
- The fatigue strength ( $S_e$ ) for  $10^{10}$  cycles is between 50 and 60 MPa at room temperature, irrespective of the type of loading. This means that stress is equal to zero.
- The high-cycle fatigue strength ( $S_e$ ) of copper increases as the temperature decreases. At low cycles, the temperature also affects the fatigue strength ( $S_e$ ). Between the room temperature and 300 °C, there is no significant variation in a vacuum. However, above this temperature threshold, there is a significant decline in fatigue strength ( $S_e$ ).
- The fatigue strength ( $S_e$ ) of copper increases with smaller grain sizes. For UFG, the improvement decreases as the order of  $10^7$  cycles is approached. If the stresses are torsional, the improvement extends to higher cycles.
- Cold working of the copper part has a significant effect as well. The greater the degree of cold work, the greater the fatigue strength ( $S_e$ ).
- Atmosphere also has a significant effect, increasing the fatigue strength in a vacuum.

**Author Contributions:** Conceptualization, E.J.-R., R.L.-L. and C.B.-L.; methodology, E.J.-R.; software, E.J.-R.; investigation, E.J.-R. and R.L.-L.; writing—original draft preparation, E.J.-R.; writing—review and editing, R.L.-L. and C.B.-L.; supervision, R.L.-L. and C.B.-L. All authors have read and agreed to the published version of the manuscript.

**Funding:** This research received no external funding.

**Data Availability Statement:** The data presented in this study are available on request from the corresponding author.

**Conflicts of Interest:** The authors declare no conflicts of interest.

## Nomenclature

|                             |  |
|-----------------------------|--|
| ETP                         | Electrolytic tough-pitch   |
| OFE                         | Oxygen-free electronic   |
| OF                          | Oxygen-free  |
| OFHC                        | Oxygen-free high-conductivity  |
| Cu-DHP                      | Phosphorus-deoxidized copper (high residual phosphorus)              |
| S-N                         | Stress–life  |
| $\sigma$                    | Stress   |
| $\sigma_{\text{max}}$       | Maximum stress   |
| $\sigma_{\text{min}}$       | Minimum stress   |
| $\sigma_m$                  | Mean stress = $(\sigma_{\text{max}} + \sigma_{\text{min}})/2$        |
| $\sigma_a$                  | Alternating stress = $(\sigma_{\text{max}} - \sigma_{\text{min}})/2$ |
| $S_e$                       | Fatigue strength   |
| $S_{e(10^8)}$               | Fatigue strength at $10^8$ cycles                                    |
| $S_{yp}$                    | Yield strength   |
| $S_{ut}$                    | Ultimate strength  |
| $\epsilon_{\text{plastic}}$ | Plastic strain amplitude   |
| $\epsilon_{\text{elastic}}$ | Elastic strain amplitude   |
| $\epsilon_{\text{Total}}$   | Total strain amplitude   |
| $\epsilon$ -N               | Strain–life  |
| R                           | Stress ratio (min/max)   |

## References

1. Wöhler, A. Results of tests made in the central workshop of the Niederschlesisch-Märkischen Eisenbahn at Frankfurt a.d.O., on the relative strength of iron, steel and copper. *Z. Bauw.* **1866**, *16*, 67–83.
2. Sun, Y.; Li, T.; Lan, L.; Chen, J.; Zhu, W.; Xue, S.; Jin, L. A Mini-Review on the Thermal Fatigue Properties of Copper Materials Applied at the Front-End of Synchrotron Radiation Facilities. *Entropy* **2023**, *25*, 714. [[CrossRef](#)] [[PubMed](#)]
3. Bathias, C. Piezoelectric Fatigue Testing Machines and Devices. *Int. J. Fatigue* **2006**, *28*, 1438–1445. [[CrossRef](#)]
4. Valiev, R.Z.; Langdon, T.G. Principles of Equal-Channel Angular Pressing as a Processing Tool for Grain Refinement. *Prog. Mater. Sci.* **2006**, *51*, 881–981. [[CrossRef](#)]
5. Design of Rotating Electrical Machines. Wiley. Available online: <https://www.wiley.com/en-us/Design+of+Rotating+Electrical+Machines-p-9780470740088> (accessed on 6 December 2023).
6. Louthan, M.R. Hydrogen Embrittlement of Metals: A Primer for the Failure Analyst. *J. Fail. Anal. Prev.* **2008**, *8*, 289–307. [[CrossRef](#)]
7. Deutsches Kupferinstitute Cu-DHP.pdf. Available online: <https://kupfer.de/wp-content/uploads/2019/11/Cu-DHP.pdf> (accessed on 5 October 2023).
8. *Data Sheet No. A6 Cu-DHP*; Conseil International Pour le Developpement du Cuivre (CIDEC): Madrid, Spain, 1968.
9. Burghoff, H.L. Fatigue Characteristics of Some Copper Alloys. *Proc. ASTM* **1947**, *47*, 695–712.
10. Hoyt, S.L. *ASME Handbook Metals Properties*; McGraw Hill: New York, NY, USA, 1954.
11. Wieland-Werke. *Wieland-Kupferwerkstoffe: Herstellung, Eigenschaften und Verarbeitung*, 6th ed.; Wieland: Ulm, Germany, 1999.
12. Granta Copper, C12200, Hard (Phosphorus de-Oxidized Arsenical h.c Copper). Available online: <https://www.ansys.com/products/materials/materials-data-library> (accessed on 4 December 2021).
13. Park, S.; Kwon, H.H.; Koo, J.M.; Seok, C.S.; Jung, D.H.; Mo, J.Y. A Study on the Fatigue Life Prediction for Bending Pipe. *Adv. Mater. Res.* **2012**, *415–417*, 2219–2225. [[CrossRef](#)]
14. Murphy, M.C. The Engineering Fatigue Properties of Wrought Copper. *Fatigue Fract. Eng. Mater. Struct.* **1981**, *4*, 199–234. [[CrossRef](#)]
15. Grover, H.J.; Institute, B.M. *Fatigue of Metals and Structures*; U.S. Government Printing Office: Washington, DC, USA, 1960.
16. Budynas, R.G.; Nisbett, J.K. *Shigley's Mechanical Engineering Design*; McGraw Hill: New York, NY, USA, 2019; ISBN 978-0-07-339821-1.
17. WebPlotDigitizer. Extract Data from Plots, Images, and Maps. Available online: <https://automeris.io/WebPlotDigitizer/> (accessed on 4 November 2023).
18. Rstudio Home Page. Available online: <https://posit.co/products/open-source/rstudio/> (accessed on 4 December 2023).
19. R: The R Project for Statistical Computing. Available online: <https://www.r-project.org/> (accessed on 1 November 2023).
20. Tahmasbi, K.; Alharthi, F.; Webster, G.; Haghshenas, M. Dynamic Frequency-Dependent Fatigue Damage in Metals: A State-of-the-Art Review. *Forces Mech.* **2023**, *10*, 100167. [[CrossRef](#)]
21. Marti, N.; Favier, V.; Gregori, F.; Saintier, N. Correlation of the Low and High Frequency Fatigue Responses of Pure Polycrystalline Copper with Mechanisms of Slip Band Formation. *Mater. Sci. Eng. A* **2020**, *772*, 138619. [[CrossRef](#)]
22. Fintová, S.; Kuběna, I.; Chlupová, A.; Jambor, M.; Šulák, I.; Chlup, Z.; Polák, J. Frequency-Dependent Fatigue Damage in Polycrystalline Copper Analyzed by FIB Tomography. *Acta Mater.* **2021**, *211*, 116859. [[CrossRef](#)]
23. Stanzl-Tschegg, S.E. Influence of Material Properties and Testing Frequency on VHCF and HCF Lives of Polycrystalline Copper. *Int. J. Fatigue* **2017**, *105*, 86–96. [[CrossRef](#)]
24. Phung, N.-L. Fatigue Sous très Faibles Amplitudes de Contrainte: Analyse des Mécanismes Précurseurs de L'amorçage de Fissures dans le Cuivre Polycristallin. Ph.D. Thesis, Ecole Nationale Supérieure d'arts et Métiers—ENSAM, Paris, France, 2012.
25. Singh, B.N.; Toft, P.; Stubbins, J.F. *Fatigue Performance of Copper and Copper Alloys before and after Irradiation with Fission Neutrons: (ITER R & D Task No. T213)*; Risø National Laboratory: Roskilde, Denmark, 1997; ISBN 978-87-550-2313-0.
26. Lukáš, P.; Kunz, L. Effect of Grain Size on the High Cycle Fatigue Behaviour of Polycrystalline Copper. *Mater. Sci. Eng.* **1987**, *85*, 67–75. [[CrossRef](#)]
27. Collini, L. *Copper Alloys—Early Applications and Current Performance—Enhancing Processes*; InTech: London, UK, 2012; ISBN 978-953-51-0160-4.
28. Goto, M.; Han, S.Z.; Yakushiji, T.; Kim, S.S.; Lim, C.Y. Fatigue Strength and Formation Behavior of Surface Damage in Ultrafine Grained Copper with Different Non-Equilibrium Microstructures. *Int. J. Fatigue* **2008**, *30*, 1333–1344. [[CrossRef](#)]
29. Khatibi, G.; Horky, J.; Weiss, B.; Zehetbauer, M.J. High Cycle Fatigue Behaviour of Copper Deformed by High Pressure Torsion. *Int. J. Fatigue* **2010**, *32*, 269–278. [[CrossRef](#)]
30. Li, R.H.; Zhang, Z.J.; Zhang, P.; Zhang, Z.F. Improved Fatigue Properties of Ultrafine-Grained Copper under Cyclic Torsion Loading. *Acta Mater.* **2013**, *61*, 5857–5868. [[CrossRef](#)]
31. Lukáš, P.; Kunz, L.; Svoboda, M. Fatigue Mechanisms in Ultrafine-Grained Copper. *Kov. Mater.* **2009**, *47*, 1–9.
32. Lukáš, P.; Kunz, L.; Svoboda, M. Overview of Fatigue Behaviour of Ultrafine-Grained Copper Produced by Severe Plastic Deformation. *Mater. Sci. Forum* **2008**, *567–568*, 9–16. [[CrossRef](#)]
33. Mughrabi, H. Fatigue, an Everlasting Materials Problem—Still En Vogue. *Procedia Eng.* **2010**, *2*, 3–26. [[CrossRef](#)]
34. Thompson, A.W.; Backofen, W.A. The Effect of Grain Size on Fatigue. *Acta Metall.* **1971**, *19*, 597–606. [[CrossRef](#)]
35. Vinogradov, A.; Hashimoto, S. Multiscale Phenomena in Fatigue of UltraFine Grain Materials—An Overview. *Mater. Trans.* **2001**, *42*, 74–84. [[CrossRef](#)]

36. Mughrabi, H.; Höppel, H.W.; Kautz, M. Fatigue and Microstructure of Ultrafine-Grained Metals Produced by Severe Plastic Deformation. *Scr. Mater.* **2004**, *51*, 807–812. [CrossRef]
37. Carstensen, J.V. *Structural Evolution and Mechanisms of Fatigue in Polycrystalline Brass*; Risø National Laboratory: Roskilde, Denmark, 1998.
38. Thompson, N.; Wadsworth, N.; Louat, N.X. The Origin of Fatigue Fracture in Copper. *Philos. Mag. A J. Theor. Exp. Appl. Phys.* **1956**, *1*, 113–126. [CrossRef]
39. Duquette, D.J. *Environmental Effects on General Fatigue Resistance and Crack Nucleation in Metals and Alloys*; DTIC: Fort Belvoir, VA, USA, 1978.
40. Mughrabi, H. On the Life-Controlling Microstructural Fatigue Mechanisms in Ductile Metals and Alloys in the Gigacycle Regime. *Fatigue Fract. Eng. Mater. Struct.* **1999**, *22*, 633–641. [CrossRef]
41. Wang, Z.; Nian, T.; Ryding, D.; Kuzay, T.M. Low-Cycle-Fatigue Behavior of Copper Materials and Their Use in Synchrotron Beamline Components. *Nucl. Instrum. Methods Phys. Res. Sect. A Accel. Spectrometers Detect. Assoc. Equip.* **1994**, *347*, 651–656. [CrossRef]
42. Simon, N.J.; Drexler, E.S.; Reed, R.P. *Properties of Copper and Copper Alloys at Cryogenic Temperatures*; National Institute of Standards and Technology: Gaithersburg, MD, USA, 1992; p. NIST MONO 177.
43. ASME—ANSI B106.1M. Design of Transmission Shafting (Second Printing). GlobalSpec. Available online: <https://standards.globalspec.com/std/709086/ANSI%20B106.1M> (accessed on 6 December 2023).
44. Soderberg, C.R. Factor of Safety and Working Stress. *Trans. Am. Soc. Mech. Eng.* **2023**, *52*, 13–21. [CrossRef]
45. Haigh, B.P. Experiments on the Fatigue of Brasses. *J. Inst. Met.* **1917**, *18*, 55–86.
46. Tamiya, Y. Low-Cycle Fatigue Fracture Phenomenon of Bended Copper Pipes under Internal Pressure. *J. Soc. Mater. Sci. Jpn.* **2012**, *61*, 550–555. [CrossRef]
47. Harun, M.F.; Mohammad, R. Fatigue Properties of JIS H3300 C1220 Copper for Strain Life Prediction. *AIP Conf. Proc.* **2018**, *1958*, 020001. [CrossRef]
48. Neuber, H. Theory of Stress Concentration for Shear-Strained Prismatical Bodies With Arbitrary Nonlinear Stress-Strain Law. *J. Appl. Mech.* **1961**, *28*, 544–550. [CrossRef]
49. Pan, X.; Wu, X.; Fu, G.; Stubbins, J.F. Grain Size Effect on Room Temperature Fatigue and Creep-Fatigue Behavior of OFHC Copper. *Fusion Sci. Technol.* **2007**, *52*, 521–525. [CrossRef]
50. Coffin, L.F. Fatigue at High Temperature—Prediction and Interpretation. *Proc. Inst. Mech. Eng.* **1974**, *188*, 109–127. [CrossRef]
51. Takahashi, S.; Sano, M.; Watanabe, A.; Kitamura, H. Prediction of Fatigue Life of High-Heat-Load Components Made of Oxygen-Free Copper by Comparing with Glidcop. *J. Synchrotron. Radiat.* **2013**, *20*, 67–73. [CrossRef] [PubMed]
52. Papavinasam, S. Chapter 5—Mechanisms. In *Corrosion Control in the Oil and Gas Industry*; Papavinasam, S., Ed.; Gulf Professional Publishing: Boston, MA, USA, 2014; pp. 249–300. ISBN 978-0-12-397022-0.
53. Briant, C.L.; Banerji, S.K. *Embrittlement of Engineering Alloys*, 1st ed.; Elsevier: Amsterdam, The Netherlands, 1983; Available online: <https://shop.elsevier.com/books/embrittlement-of-engineering-alloys/briant/978-0-12-341825-8> (accessed on 26 October 2023).
54. Lynch, S.P. 18—Failures of Structures and Components by Metal-Induced Embrittlement. In *Stress Corrosion Cracking*; Raja, V.S., Shoji, T., Eds.; Woodhead Publishing Series in Metals and Surface Engineering; Woodhead Publishing: Sawston, UK, 2011; pp. 714–748. ISBN 978-1-84569-673-3.
55. Norkett, J.E.; Dickey, M.D.; Miller, V.M. A Review of Liquid Metal Embrittlement: Cracking Open the Disparate Mechanisms. *Met. Mater. Trans. A* **2021**, *52*, 2158–2172. [CrossRef]
56. Duffner, D.H. Air Conditioner Failure Investigation—Intergranular Cracking in a Pure Copper Condenser Tube. *J. Fail. Anal. Prev.* **2005**, *5*, 79–85. [CrossRef]
57. McDougal, J.L.; Stevenson, M.E. Stress-Corrosion Cracking in Copper Refrigerant Tubing. *J. Fail. Anal. Prev.* **2005**, *5*, 13–17. [CrossRef]
58. Stevenson, M.E.; McDougall, J.L.; Barkey, M.E. Stresses in Bent Copper Tubing: Application to Fatigue and Stress-Corrosion Cracking Failure Mechanisms. *J. Fail. Anal. Prev.* **2005**, *5*, 25–29. [CrossRef]
59. Pantazopoulos, G. Metallurgical Observations on Fatigue Failure of a Bent Copper Tube. *J. Fail. Anal. Prev.* **2009**, *9*, 270–274. [CrossRef]
60. Pantazopoulos, G.; Zormalia, S.; Vazdirvanidis, A. Failure Analysis of a Copper Tube in an Industrial Refrigeration Unit: A Case History. *Int. J. Struct. Integr.* **2013**, *4*, 55–66. [CrossRef]
61. Miyamoto, H.; Saburi, D.; Fujiwara, H. A Microstructural Aspect of Intergranular Stress Corrosion Cracking of Semi-Hard U-Bend Tubes of Commercially Pure Copper in Cooling Systems. *Eng. Fail. Anal.* **2012**, *26*, 108–119. [CrossRef]
62. Kim, S.Y.; Kim, H.I.; Seok, C.S.; Lee, J.K.; Mo, J.Y.; Park, D.Y. Evaluation of Tensile Properties and Bending-Induced Residual Stress of Slender Copper Pipe. *Key Eng. Mater.* **2006**, 321–323, 636–639. [CrossRef]
63. Kim, S.-Y.; Koo, J.-M.; Seok, C.-S. Evaluation of Residual Stress of Copper Pipe by Using Raman Spectroscopy. *Mod. Phys. Lett. B* **2008**, *22*, 1007–1012. [CrossRef]

- 
64. Harlow, D.G. Statistically Modeling the Fatigue Life of Copper and Aluminum Wires Using Archival Data. *Metals* **2023**, *13*, 1419. [[CrossRef](#)]
  65. Tanaka, T.; Sugioka, T.; Kobayashi, T.; Shohji, I.; Shimada, Y.; Watanabe, H.; Kamakoshi, Y. Low Cycle Fatigue Characteristics of Oxygen-Free Copper for Electric Power Equipment. *Materials* **2021**, *14*, 4237. [[CrossRef](#)] [[PubMed](#)]

**Disclaimer/Publisher's Note:** The statements, opinions and data contained in all publications are solely those of the individual author(s) and contributor(s) and not of MDPI and/or the editor(s). MDPI and/or the editor(s) disclaim responsibility for any injury to people or property resulting from any ideas, methods, instructions or products referred to in the content.